Biochimica et Biophysica Acta 1838 (2014) 2140–2148

Contents lists available at ScienceDirect

Biochimica et Biophysica Acta

journal homepage: www.elsevier.com/locate/bbamem

Membrane interactions and biological activity of antimicrobial peptides from Australian scorpion ☆

Karen Luna-Ramírez [a,b], Marc-Antoine Sani [c], Jesus Silva-Sanchez [d], Juana María Jiménez-Vargas [e], Fernando Reyna-Flores [d], Kenneth D. Winkel [a], Christine E. Wright [a,b], Lourival D. Possani [e,*], Frances Separovic [c,*]

[a] Australian Venom Research Unit, Department of Pharmacology, University of Melbourne, Victoria 3010, Australia
[b] Cardiovascular Therapeutics Unit, Department of Pharmacology, University of Melbourne, Victoria 3010, Australia
[c] School of Chemistry, Bio21 Institute, University of Melbourne, Melbourne, VIC 3010, Australia
[d] Instituto Nacional de Salud Pública, Centro de Investigación sobre Enfermedades Infecciosas, Avenida Universidad 655, Cuernavaca, Morelos 62508, Mexico
[e] Departamento de Medicina Molecular y Bioprocesos, Instituto de Biotecnología, Universidad Nacional Autónoma de México, Avenida Universidad, 2001, Colonia Chamilpa, Apartado Postal 510-3, Cuernavaca 62210, Mexico

ARTICLE INFO

Article history:
Received 27 August 2013
Received in revised form 13 October 2013
Accepted 29 October 2013
Available online 4 November 2013

Keywords:
Antimicrobial peptide
Membrane interaction
Phospholipid
Dye release
Hemolysis
Antibiotic

ABSTRACT

UyCT peptides are antimicrobial peptides isolated from the venom of the Australian scorpion. The activity of the UyCT peptides against Gram positive and Gram negative bacteria and red blood cells was determined. The membrane interactions of these peptides were evaluated by dye release (DR) of the fluorophore calcein from liposomes and isothermal titration calorimetry (ITC); and their secondary structure was determined by circular dichroism (CD). Three different lipid systems were used to mimic red blood cells, *Escherichia coli* and *Staphylococcus aureus* membranes. UyCT peptides exhibited broad spectrum antimicrobial activity with low MIC for *S. aureus* and multi-drug resistant Gram negative strains. Peptide combinations showed some synergy enhancing their potency but not hemolytic activity. The UyCT peptides adopted a helical structure in lipid environments and DR results confirmed that the mechanism of action is by disrupting the membrane. ITC data indicated that UyCT peptides preferred prokaryotic rather than eukaryotic membranes. The overall results suggest that UyCT peptides could be pharmaceutical leads for the treatment of Gram negative multiresistant bacterial infections, especially against *Acinetobacter baumanni*, and candidates for peptidomimetics to enhance their potency and minimize hemolysis. This article is part of a Special Issue entitled: Interfacially Active Peptides and Proteins. Guest Editors: William C. Wimley and Kalina Hristova.

1. Introduction

The widespread use of antibiotics has contributed to the emergence of multi-resistant bacteria as a major public health problem, leading to untreatable infections and nosocomial infections becoming a critical problem [1]. The evolution and spread of new resistant strains to conventional antibiotics (*e.g.* MRSA, *Enterococcus* spp., *Acinetobacter baumannii*) is of particular interest. Focus is on Gram-negative bacteria resistant to oral antibiotics and those forming biofilms. A means of managing these is to develop novel drugs to which resistance mechanisms are less likely to evolve. In the past decades, naturally occurring antimicrobial peptides (AMP) from insects, arachnids and some vertebrates have shown promising activities, representing both an opportunity and a challenge for pharmacological development.

AMP usually consist of 13 to 50 amino acids and generally α-helical, amphipathic, positively charged membrane-acting molecules [2]. They are ribosomally synthesized and often have post-translational modifications. AMP are key components of innate immunity and, therefore, show promise as antibacterial agents. AMP are active against a broad spectrum of pathogens (bacteria, fungi, parasites and viruses) and, generally, inhibit pathogens quickly, although their mode of action presents a problem — toxicity. Nevertheless, there is potential since their mechanism of action is to disrupt the bacterial membrane so that bacteria are less likely to evolve or gain resistance.

The Antimicrobial Peptide Database (http://aps.unmc.edu/AP/main.php accessed 24 Aug 2013) contains more than 2200 AMP from different sources [3]. Despite this growing library, the relationship between their amino-acid sequences and bactericidal activity remains to be elucidated. AMP are classified into three major groups: (i) linear cysteine-free peptides with an α-helical conformation (insect cecropins, magainins,

Abbreviations: AMP, antimicrobial peptides; Chol, cholesterol; CD, circular dichroism; DR, dye release; ITC, isothermal titration calorimetry; LPC, lipopolysaccharide; LUV, large unilamellar vesicles; MDR, multi-drug resistant; MIC, minimum inhibitory concentration; MRE, mean-residue ellipticity; POPC, palmitoyloleoyl-phosphatidylcholine; POPE, palmitoyloleoyl-phosphatidylethanolamine; POPG, palmitoyloleoyl-phosphatidylglycerol; RBC, red blood cell; TOCL, tetraoeloyl-cardiolipin

☆ This article is part of a Special Issue entitled: Interfacially Active Peptides and Proteins. Guest Editors: William C. Wimley and Kalina Hristova.

* Corresponding authors.
E-mail addresses: possani@ibt.unam.mx (L.D. Possani), fs@unimelb.edu.au (F. Separovic).

0005-2736/$ – see front matter © 2013 Elsevier B.V. All rights reserved.
http://dx.doi.org/10.1016/j.bbamem.2013.10.022

etc.) [4], (ii) cyclic and open-ended cyclic peptides with one to four disulfide bridges (defensins, protegrin, *etc.*), and (iii) peptides with an over-representation of some amino acids (proline rich, glycine rich, histidine rich, *etc.*) [5]. This report focuses on the first group of AMP.

Linear amphipathic α-helical AMP are present in invertebrates (insects and tunicates) and vertebrates, including humans [6]. Generally, they are potent broad-spectrum antimicrobials with a hemolytic tendency. Cecropin, from the moth *Hyalophora cecropia*, was one of the first α-helical AMP to be discovered [7]. Subsequently, cecropins from tunicate and nematodes were also identified. Mature cecropin peptides are cysteine-free AMP of 35–39 amino acids forming two linear α-helices connected by a hinge, which integrate into the anionic cell membranes of bacteria leading to their disruption [8]. Cecropins have two major characteristics: a tryptophan residue in position 1 or 2, and an amidated C-terminus.

AMP isolated from the venom gland of arthropods are well represented by melittin, a major component of bee venom found to be bactericidal by Schmidt-Lange in 1941 [9], and ponericins isolated from the predatory ant *Pachycondylas goeldii* [10]. Ponericins are highly similar to cecropins (60% sequence similarity) and have the tryptophan signature, but lack the C-terminal amidation.

AMP from spiders and scorpions have also been identified. Oxyopinins and cupiennins from the wolf spider *Oxyopes kitabensis* and hunting spider *Cupiennius salei*, respectively, possess anti-bacterial, hemolytic and insecticidal properties [11,12]. Oxyopinins share sequence similarities to ponericins and to the dermaseptins, α-helical AMP from amphibian skin [13]. Cupiennins are characterized by a hydrophobic N-terminal region, a C-terminus composed of polar and charged residues, and an amidated glutamic acid residue [14].

Only a few AMP from scorpion venom have been described. So far, only 27 AMP have been reported from 14 different scorpion species [15–19]. Antimicrobial peptides from scorpions are a class of scorpion peptides recently classified as non-disulfide bridges peptides (NDBP), very different from the neurotoxic peptides isolated from this species. AMP from scorpions can inhibit the growth of a wide-range of microorganisms including viruses, Gram-positive and Gram-negative bacteria, protozoa, yeast and fungi; these AMP may also be hemolytic and cytotoxic to cancer cells [18]. Their mode of action is not yet clear but they appear to disturb membranes by forming transient pores, enhancing membrane permeability, which leads to leakage of cell contents and death [20].

In an effort to investigate novel antibiotics, AMP found in the venom of the Australian scorpion *Urodacus yaschenkoi* [21] have been studied. The peptides described herein, UyCT1, UyCT3 and UyCT5, are short naturally occurring cationic peptides that are active against Gram-positive and Gram-negative bacteria. UyCT2 is an analog of UyCT1.

These four peptides and binary mixtures were studied to understand the relationship between the amino acid sequence (activity) and membrane lipid composition. *In vitro* bioassays against multidrug resistant (MDR) bacteria from clinical isolates were performed to determine the minimum inhibitory concentration (MIC) and to identify a preferential bacterial target. Also, the hemolytic activity of these peptides was determined to assess their interaction with eukaryotic cells. Furthermore, their secondary structure was determined by CD, their capacity to permeate membranes by dye release (DR) of the fluorophore calcein from liposomes, and their affinity for specific lipid membranes was assessed by isothermal titration calorimetry (ITC). These experiments were designed to shed light on the molecular mechanism by which these peptides trigger antibacterial activity. This study was carried out using phospholipid bilayers with large unilamellar vesicles (LUV, 100 nm diameter) mimicking human red blood cells (POPC/Chol), *Escherichia coli* (POPE/POPG) and *Staphylococcus aureus* (POPG/TOCL) membranes. To confirm membrane targeting by these peptides, D-isomers of UyCT peptides were synthesized and assayed.

2. Materials and methods

2.1. Materials

Peptides UyCT1, UyCT2, UyCT3 and UyCT5 (Genbank JX274240.1, JX274241.1, JX274242.1) were synthesized by Biomatik Corporation (Ontario, Canada) and delivered 98% pure (after TFA removal). The molecular weights of the pure peptides were confirmed by mass spectrometry. Palmitoyloleoyl-phosphatidylcholine (POPC), palmitoyloleoyl-phosphatidylethanolamine (POPE), palmitoyloleoyl-phosphatidylglycerol (POPG) and tetraoeloyl-cardiolipin (TOCL) phospholipids were purchased from Avanti Polar Lipids (Alabaster, USA) and were used without further purification. Calcein, Aprotonin (A3886), Triton-X100 and Sephadex G-100 gel filtration media were purchased from Sigma (St Louis, USA).

Multi-drug resistant (MDR) clinical isolates used herein were obtained from the Center for Research on Infectious Diseases bacterial collection of the National Institute of Public Health, Cuernavaca (Morelos, Mexico) and included: *E. coli*, 170 [22], 09-280, 5509, 09-240 [23]; *Klebsiella pneumoniae* 01-239, 01-252 [23,24]; *Enterobacter cloacae* 14-262, 06-26 [23]; *A. baumannii* 5821; *Pseudomona aeruginosa* 5106, 3599 [25]; and *S. aureus* 01-001, 06-051. These clinical isolates were collected from different patients from 14 hospitals in nine major cities in Mexico during June 2002 to November 2009. In all cases, the species of the organisms and susceptibility patterns were determined with a Dade Micro-Scan combo PC-20 assay for Gram-positive and NC-33 for Gram-negative bacteria (Siemens Healthcare Diagnostics Inc., West Sacramento, USA).

2.2. Susceptibility tests

2.2.1. Minimum Inhibitory Concentration (MIC) assays

The determination of the MIC for different peptides was performed using the broth microdilution method following the Clinical and Laboratory Standards Institute (CSLI) guidelines. MIC was determined as the lowest concentration of the compound that completely inhibited bacterial growth. Briefly, the bacterial cultures were grown in Mueller-Hinton broth medium (100 μL) in 96-well ELISA plates. Each well contained 5 μL of bacterial culture with 5×10^4 CFU/mL and the appropriate amount of the AMP to be tested. Dilutions of the peptides based on two-fold dilution, typically 2–64 μM, were prepared by dissolving the dried peptides in distilled water and tested in duplicate. Microbial growth inhibition was observed after incubation for 16–18 h at 35 °C. As reference strains, *E. coli* ATCC 25922, *P. aeruginosa* ATCC 27853 and *S. aureus* ATCC 29213 were used. Experiments were performed with different clinical isolates causing nosocomial infections: *E. coli* (4 isolates), *K. pneumoniae* (2 isolates), *E. cloacae* (3 isolates), *P. aeruginosa* (2 isolates), *A. baumannii* (1 isolate) and *S. aureus* (2 isolates). Subsequent experiments were performed with intermediate concentrations to determine the MIC of each peptide and their combinations.

2.2.2. Hemolytic assays

The hemolytic activity was assessed by incubating (at 37 °C for 1 h) a suspension of human erythrocytes (7×10^7 cells/mL) in phosphate buffered saline (PBS) from a healthy donor with increasing concentrations of each peptide or combination of peptides. The samples were centrifuged for 5 min at 2000*g* and the release of hemoglobin was monitored by measuring the absorbance of the supernatant at 570 nm in a NanoDrop 1000 spectrophotometer (Thermo Fisher Scientific, Wilmington, USA). [For details see [21,26]]. All peptide concentrations were tested in quadruplicate and the data expressed as mean ± SD. Percentage of hemolysis was calculated using the following formula: % hemolysis = 100 $(A_{peptide} - A_{PBS})/(A_{triton} - A_{PBS})$. The zero and 100% hemolysis values were determined in PBS and 10% Triton X100, respectively. The peptide concentrations that cause 50% hemolysis of human erythrocytes (HC_{50}) were obtained using a non-linear

regression analysis, where the data were fitted with a logistical sigmoidal equation using the software package Origin 7 (Microcal Inc., USA).

2.3. Circular dichroism (CD) experiments

2.3.1. CD sample preparation

Peptides UyCT1 and UyCT2 were dissolved in 20 mM phosphate and 5 mM NaCl buffer solution (pH 7.0). UyCT3 and UyCT5 showed higher solubility in Milli-Q water. For all peptides, stock solutions containing 1 mg/mL were made. The stock solution was sonicated (10 s) and vortexed prior to each use. To prepare binary vesicles, lipids were co-solubilized in chloroform/methanol (3:1, v/v) before removal of solvents by rotatory evaporation. Lipids were hydrated in Milli-Q water and lyophilized over-night. The resultant lipid powders were re-suspended in 20 mM phosphate and 5 mM NaCl buffer solution (pH 7.0) The homogeneous solution was then extruded 10 times through an Avanti Mini-Extruder (Alabaster, USA) using 100 nm polycarbonate filters to produce LUV of 100 nm diameter. The size of the LUV was confirmed by dynamic light scattering (DLS) performed on a Nano Zetasizer (Malvern Instruments Ltd, UK). Appropriate volumes of peptide stock solution and lipid vesicle dispersion were mixed to produce 160 μL samples with a fixed peptide concentration of 50 μM.

2.3.2. CD measurements

CD spectra were acquired on a Chirascan spectropolarimeter (Applied Photophysics Ltd, UK) between 180 and 260 nm using a 0.1 mm path-length cylindrical quartz cell (Starna, Hainault, UK). Spectra were acquired with 1 nm data intervals, 1 s integration time and 3 scan accumulation. Signal was recorded as milli-degrees at 25 °C.

2.3.3. CD spectral deconvolution

Spectra were zeroed at 260 nm and normalized to give units of mean-residue ellipticity (MRE) according to $[\theta]\ \mathrm{MRE} = \theta/(c \times l \times N_r)$, where θ is the recorded ellipticity in milli-degrees, c is the peptide concentration in $\mathrm{dmol.L^{-1}}$, l is the cell path-length in cm, and N_r is the number of residues per peptide. The secondary structure was calculated from processed CD spectra using the DICHROWEB [27] website with the ContinLL algorithm and the SMP56 basis-set [28].

2.4. Dye release assay

2.4.1. Calcein solution preparation

Calcein was initially insoluble in water and was, therefore, dissolved in 4 eq. NaOH. The resultant solution was vortexed extensively until dissolution was complete. Appropriate volumes of Tris and NaCl were added to the calcein solution before pH adjustment back to 7.3 with HCl to yield a final solution of 80 mM calcein in 30 mM Tris and 20 mM NaCl.

2.4.2. Calcein encapsulation in Large Unilamellar Vesicles (LUV)

To prepare calcein-loaded LUV, lipids were suspended in 250 μL of a dye solution made of 80 mM calcein, Tris 30 mM (pH 7.3) and 20 mM NaCl. The solutions were freeze/thaw five times and then extruded 10 times through an Avanti Mini-Extruder (Alabaster, USA) using 0.1 μm polycarbonate filters to produce LUV of nominal 100 nm diameter. Separation from free dye was obtained by gel filtration using Sephadex G-100 column media. The gel media and running buffer were carefully degassed before use to prevent air bubbles forming in the column. Samples were eluted under gravity with 30 mM Tris and 100 mM NaCl (pH 7.3) running buffer solution at ~1.5 mL/min. Approximately 0.75 mL fractions were collected, with the two most concentrated fractions pooled prior to lipid concentration determination. Phospholipid concentrations were determined in triplicate by phosphorus assay [29]. In parallel, lipids were also suspended in a calcein-free buffer to produce similar LUV solutions. The diameter of the calcein-free LUV was determined by DLS measurements using a Nano Zetasizer.

2.4.3. Dye release measurements

Samples containing different lipid to peptide molar ratio from 1 to 500 were prepared with a final volume of 400 μL. Each sample contained 250 μM of lipid but only half of the LUV had dye-encapsulated. Samples were incubated for 30 min at room temperature prior to measurement. Positive control (or 100% fluorescence) was obtained by adding Triton-X100 and negative control (baseline fluorescence) by adding buffer. Measurements were made at room temperature using a Varian Cary Eclipse spectrophotometer (Melbourne, Australia) using a semi-micro quartz cell (Starna, Hainault, UK). The excitation wavelength was 490 nm with a 2.5 nm width and the emission fluorescence was recorded between 500 and 600 nm with a 2.5 nm width. Triplicate measurements were averaged and the percentage of fluorescence was calculated using the equation:

$$\%\mathrm{fluorescence} = \frac{I - I_0}{I_{max} - I_0} \times 100 \quad (1)$$

where I is the fluorescence obtained, I_0 is the baseline fluorescence, and I_{max} is the maximum fluorescence obtained with addition of Triton-X100. The error bars were calculated from the partial derivatives of Eq. (1) and the standard deviations obtained from the triplicate experiments.

The percentages *versus* the peptide concentration (log scale) plots were fitted using a concentration–response equation:

$$y = y_0 + \frac{(y_{max} - y_0)}{1 + \left(\frac{x}{AC_{50}}\right)^n} \quad (2)$$

where y_0 is the minimum fluorescence obtained at the highest lipid to peptide molar ratio (fixed), y_{max} is the maximum obtained after addition of Triton-X100 (fixed), *x* is log[peptide], AC_{50} represents the concentration necessary to produce half of the maximum fluorescence, and n – the Hill coefficient – is representative of the cooperativity between the peptides to produce the activity.

3. Results and discussion

3.1. MIC and hemolytic activity

The antibiotic activity of the peptides was assayed against MDR clinical isolates causing nosocomial infections to determine their MIC. Three reference strains, which are susceptible to antibiotics, *E. coli* ATCC25922, *P. aeruginosa* 27853 and *S. aureus* ATCC29213, were included in the screening. Also, their activity was compared to the antibiotics ampicillin and sulfonamide. Peptides were assayed up to 32 μM because above that concentration the hemolytic activity was greater than 50%, although not for UyCT2. Table 1 shows the MIC results with the peptide sequences given in Table 2. UyCT2 was the least potent AMP tested herein, showing no activity towards Gram-negative bacteria up to 32 μM. The MIC values determined for this peptide were ≥32 μM for all bacterial cultures, but for *E. coli* and *S. aureus* control strains, UyCT2 was more active than ampicillin (MIC 58 μM). In addition, all UyCT AMP failed to inhibit the growth of *P. aeruginosa* cultures at 32 μM.

UyCT3 and UyCT5 shared similar behavior, which is not surprising due to their similar sequences. Their MIC was in the range 30–32 μM for almost all strains but, interestingly, for *A. baumannii* was 10 μM and 14 μM, respectively, whereas ampicillin was >16 μM. For *S. aureus* – the only Gram positive bacteria studied herein – the MIC for UyTC3 and UyCT5 was significantly lower than for the others strains being 4–8 or 2–4 μM, respectively.

UyCT1 was the most potent broad-spectrum AMP in this study with MIC for MDR *E. coli* of 14 μM, *K. pneumoniae* 12 μM, *E. cloacae* 14 μM, *A. baumannii* 7 μM and for *S. aureus* 4 μM. In all cases, UyCT1 was more potent than ampicillin.

Table 1
MIC of AMP and antibiotics against antibiotic susceptible bacteria as reference strains (r) and multi-resistant clinical isolates. Each test was performed in duplicate.

Genus	Clinical isolate	MIC (μM)					
		UyCT1	UyCT2	UyCT3	UyCT5	Ampicillin	Sulfonamide
E. coli (r)	**25922***	10	45	25	25	58	nd
E. coli	170	32	>32	32	>32	nd	nd
	09-280	32	>32	32	>32	>16	38
	5509	>32	>32	>32	32	nd	nd
	09-240	14	50	30	30	>16	38
K. pneumoniae	**01-239**	12	50	30	>32	>16	>38
	01-252	32	>32	>32	>32	>16	>38
E. cloacae	06-267	32	>32	>32	>32	>16	38
	14-262	14	50	32	>32	>16	38
P. aeruginosa (r)	27853	>32	>32	>32	>32	58	nd
P. aeruginosa	5106	>32	>32	>32	>32	nd	nd
	3599	>32	>32	>32	>32	nd	nd
A. baumannii	**5821**	7	38	10	14	>16	76
S. aureus (r) (+)	29213	4	32	8	4	58	nd
S. aureus	01-001	4	>32	4	2	>8	38
	06-051	4	>32	4	2	>8	38

(r) Reference strain, nd — not done.
* Strains in bold were used for testing combinations of peptides.

S. aureus was the only Gram positive bacteria tested in this communication. All UyCT AMP, with the exception of UyCT2, exhibited the lowest MIC values towards this strain, indicating that they are more active against Gram-positive bacteria.

UyCT peptides are cationic peptides with an amphipathic nature and, therefore, may have the ability to form pores in cell membranes. Consequently their hemolytic activity was determined. Human erythrocytes were incubated with peptide concentrations within the range shown to cause bacterial inhibition (1–35 μM for combinations and 1–100 μM for single peptides).

The effective concentration that caused 50% erythrocyte lysis (HC_{50}) for single peptides [21] is shown in Table 2. The data show that UyCT peptides are mildly hemolytic at MIC concentrations. Interestingly, UyCT2 is not hemolytic but at the same time it is the least potent antimicrobial of the UyCT peptides.

3.2. Peptide combination

In an attempt to increase the potency of the peptides and decrease lysis of red blood cells, binary mixture of peptides was assayed against the MDR strains with MIC <32 μM (*i.e.*, against the MDR strains that showed higher susceptibility). The chosen combinations were UyCT5 + UyCT1, UyCT1 + UyCT3, UyCT3 + UyCT5 and UyCT2 + UyCT5. The last combination was made to assess the behavior of a non-potent and non-lytic peptide with a potent and lytic peptide. Based on the HC_{50} determined for single peptides, the concentration of the first peptide was fixed at 10 μM and the second varied from 1 to 16 μM.

The MIC results for peptide combinations (Table 3) exhibited lower values than for single peptides, suggesting synergistic or additive effects. For most cases, the MIC for peptide combinations was below 22 μM, whereas for single peptides was around 30 μM. The combination UyCT2 + UyCT5 was the least active and for some strains was not even active at the highest concentration tested in this experiment.

It should be noted that for *A. baumannii*, if the first peptide was fixed at 10 μM, the concentration combinations were not appropriate because the MIC for single peptides against this strain (Table 1) was in the range 7–14 μM (except for UyCT2). Therefore, setting a concentration of 10 μM for a given peptide already inhibits the growth of the bacteria. Hence, the fixed concentration for the first peptide was changed to 5 μM and the second peptide varied from 0.5 to 5 μM. The results (Table 4) show that UyCT peptides are potently bactericidal against *A. baumanni* and suggest a synergistic effect.

To assess an additive or synergistic interaction with the combination of peptides, the results were analyzed using a 'fixed ratio design' isobologram model [30–32]. The isobolograms consisted of an additivity line (isobole) that connects MIC_{100} of Peptide Y on the vertical axis to MIC_{100} of Peptide X on the horizontal axis. If the experimental MIC combination is a point on the isobole (or not significantly off the isobole), the interaction is merely additive. If the experimental MIC combination is off and below the isobole, there is synergism. If it is off and above the isobole there is subadditivity or antagonism. Simple additivity was defined when the combination of drugs led to a simple mathematically predictable effect. It is worth noting that these isobolograms are an adapted model from Tallarida [31] wherein, instead of using EC_{50} values, MIC_{100} values were used.

According to the isobologram model (Fig. 1), the combination of UyCT3 + UyCT5 had a clear synergistic effect for all strains tested. Surprisingly, UyCT2 + UyCT5 had a synergistic effect for *E. coli* and *A. baumannii*. For the other strains with this combination, it was not possible to accurately determine a synergistic effect because MICs were reported as an uncertain value (*e.g.* >26 μM). UyCT5 + UyCT1 showed a synergistic effect only against *E. coli* and *A. baumannii*, while the point fell on the isobole for the others strains. UyCT1 + UyCT3 only showed a synergistic effect towards *A. baumannii*. In summary, all combinations showed a synergistic effect against *A. baumannii*.

The hemolytic activity of the combination of peptides was also determined (Table 5). The data were analyzed by constructing concentration–response curves which included 4 concentrations for single and combinations of peptides. In all cases, the curve was shifted to the right (meaning the combination of peptides needed higher concentrations to reach HC_{50} than for a single peptide), highlighting that the synergy in MIC does not also occur with hemolysis. The HC_{50} for the combinations of peptides did not decrease as expected when combining two cationic amphipathic peptides. Possibly, this was due to the formation of peptide complexes or aggregates such as dimers and changing the physicochemical properties of the AMP.

Table 2
Effective concentration [21] that caused 50% erythrocyte lysis (HC_{50}).

Peptide	Amino acid sequence*	HC_{50}(μM)
UyCT1	GFWGKLWEGVKNAI	22.8 ± 1.6
UyCT2	FWGKLWEGVKNAI	>100
UyCT3	ILSAIWSGIKSLF	17.3 ± 0.8
UyCT5	IWSAIWSGIKGLL	14.1 ± 0.3

HC_{50} determination made with 2.8×10^7 cell/mL.
* Note that the C-terminal residue is amidated.

Table 3
MIC (μM) values for peptide combinations using the 'fixed ratio' design[a].

Strain	UyCT5 (10 μM) + UyCT1	UyCT1 (10 μM) + UyCT3	UyCT3 (10 μM) + UyCT5	UyCT2 (10 μM) + UyCT5
E. coli ATCC 25922	6	8	4	12
E. coli 09-240	12	12	10	>16
K. pneumoniae 01-239	12	10	14	>16
E. cloacae 14-262	12	16	>16	>16
A. baumannii 5821	<2	<1	<1	4

[a] The first listed peptide (Peptide 'A') in the combination was fixed at 10 μM.

3.3. Circular dichroism (CD)

The secondary structure of UyCT peptides in contact with large unilamellar vesicles (LUV, 100 nm diameter) of phospholipids mimicking human red blood cells (POPC/Chol), *E. coli* (POPE/POPG) and *S. aureus* (POPG/TOCL) membranes was determined using the CD technique (*e.g.* [33]).

UyCT AMP are unstructured in buffer and adopt an α-helical conformation in contact with LUV (~60% helical content) (Fig. 2 and Table 6). The CD spectrum of UyCT peptides in buffer is dominated by a minimum at ~200 nm, characteristic of the random coil conformation; while in lipid environments two minima at 208 nm and 222 nm and a maximum at 193 nm are observed indicating α-helical structures.

From the helical conformation, an α-helical wheel projection can be built showing the amphipathic character of UyCTs, a characteristic that favors antimicrobial properties against bacteria [6,34]. The wheel shows hydrophobic amino acids concentrated on one side of the helix (yellow residues), usually with polar or hydrophilic amino acids on the other (green – polar and blue – charged) (Fig. 3). This arrangement usually induces the hydrophobic side into the hydrophobic core of the lipid membrane while the charged/hydrophilic side interacts with the charged and solvent-exposed surface of the model bacterial membranes.

3.4. Dye release (DR)

The CD and HC_{50} results suggested that the AMP used in this study have a membrane-permeabilizing activity and, therefore, the amount of leakage that these peptides can produce from membranes bilayers mimicking erythrocytes and prokaryotic cells was determined. The percentage of fluorescence at 50 μM of peptide and 250 μM of lipid was analyzed to compare the behavior of these peptides (Fig. S2). In eukaryotic-like membranes all peptides but UyCT3 reached 100% release. UyCT3 only reached 85%. In *E. coli*-like membranes, the activity was less than for red blood cell (RBC)-like. The maximum release reached was for UyCT2 with 90%, then UyCT5 with 80%, UyCT1 60% and UyCT3 only 20%. For *S. aureus*-like membranes the peptides behaved similarly reaching almost 100% but UyCT3 only reached 40%. Overall, according to dye release experiments, UyCT3 was the least active peptide and the hemolytic tendency (Table 2) was corroborated by the amount of release reached with RBC-like model membranes.

The percentage of fluorescence obtained with the dye release experiments *versus* the logarithm of peptide concentration was plotted and fitted using a dose–response equation (Fig. 4 and Table 7) as a means to compare the relative potency of the four peptides toward a particular model membrane. In all three systems, 100% release was achieved except for UyCT1 and UyCT3 in *E. coli*-like membrane (POPE/POPG) which only reached ~50% release. For *S. aureus*-like membrane all but UyCT3 reached 100% release. In general, these experiments show that UyCT peptides lyse neutral more than anionic membranes, possibly due to a stronger surface interaction with the latter (as indicated by ITC data, Supplementary data).

It is interesting to note that isothermal titration calorimetry (ITC) (see Supplementary data) results showed a greater interaction with prokaryotic-like rather than eukaryotic-like model membranes: the K_d for *E. coli* and *S. aureus* mimics was in the range of 2–30 μM and for RBC was 150–200 μM (see Tables S1 and S2 in Supplementary data). The 100 fold difference shows that UyCT peptides have a preference for bacterial model membranes. The dye release experiments indicate, however, that insertion of the peptides into the model membranes is less likely.

Our model RBC membrane contains POPC and 20% cholesterol (Chol) whereas the human RBC membrane is composed of 3 layers: the glycocalyx on the exterior, rich in carbohydrates; the lipid bilayer which contains many lipids and transmembrane proteins; and the membrane skeleton, a structural network of proteins. The five major lipid membrane constituents are phosphatidylcholine (PC); sphingomyelin (SM); phosphatidylethanolamine (PE); phosphoinositol (PI) (small amounts) and phosphatidylserine (PS) [35]. Although about half of the mass in RBC membrane is proteins, the other half is lipids, mainly phospholipid and cholesterol, which we used as a mimic of the outer membrane monolayer. The model used herein is a simplistic model of the human erythrocyte membrane which appears not to reflect the HC_{50} determinations made with 'live' cells (Table 2), which show UyCT2 as the least active and not UyCT3. *i.e.*, for RBC, the HC_{50} results showed that UyCT2 is not very hemolytic whereas in the DR assay, UyCT2 reached 100% release at low concentration. UyCT3 was the least active for DR but, based on HC_{50}, it is as hemolytic as the other peptides. However, the ITC data suggest otherwise and both membrane affinity and insertion need to be considered.

Table 4
MIC against *A. baumannii* 5821 for peptide combinations using the 'fixed ratio' design[a].

Combination[a]	MIC (μM)
UyCT5 + UyCT1	1
UyCT1 + UyCT3	<0.5
UyCT3 + UyCT5	2
UyCT2 + UyCT5	>5

[a] Concentration of first peptide fixed at 5 μM.

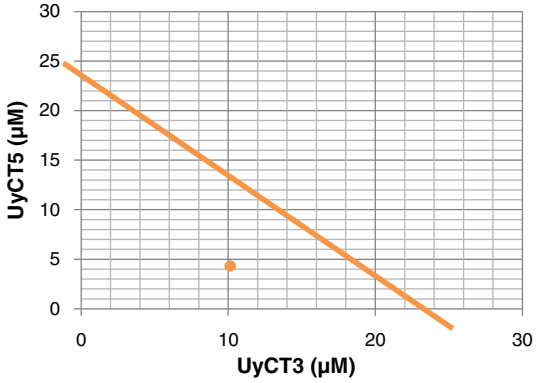

Fig. 1. Example of a 'fixed ratio design' isobologram graph showing the synergistic effect for *E. coli* 25922 with [UyCT3] fixed at 10 μM + [UyCT5]. Individual MIC_{100} for UyCT3 and UyCT5 was 25 μM. Orange line, isobologram showing theoretical line of additivity. Orange dot showing the MIC_{100} for the mixture (MIC_{100} for mixture: UyCT3 = 10 μM and UyCT5 = 4 μM) showing synergism.

Table 5
HC_{50} results[a] for peptide combinations.

Combination[b]	HC_{50} μM
UyCT5 + UyCT1	34.2 ± 1.6
UyCT1 + UyCT3	22.3 ± 0.5
UyCT3 + UyCT5	19.8 ± 0.2
UyCT2 + UyCT5	24.8 ± 0.8

[a] HC_{50} determination with 7×10^7 cell/mL.
[b] Determined from concentration–response curve (see Fig. S1).

Table 6
Helical content of UyCT peptides in LUV.

Helical percentage of UyCT peptides from CD experiments[a]				
Lipid system	UyCT1	UyCT2	UyCT3	UyCT5
POPC/Chol	65%	58%	60%	55%
POPE/POPG 7:3	60%	64%	63%	65%
POPG/TOCL 3:2	55%	66%	58%	60%

[a] Deconvolution performed with DICHROWEB using the protein database Smp10 and contin-LL algorithm. Helical content in buffer was ~7% for each peptide.

For the case of Gram-negative bacteria, POPE/POPG 7:3 was used as a membrane model without the lipopolysaccharide (LPS) or endotoxin layer which is a distinctive component of Gram-negative bacterial membranes. The MIC values for Gram-negative bacteria indicate UyCT1 as the most potent peptide, but UyCT1 only reached 50% release in the DR assay. According to the MIC results, UyCT2 was the least active against Gram-negative bacteria while the DR results showed 100% release at low concentrations. The MIC values for Gram-positive bacteria indicate that UyCT peptides are potent inhibitors of *S. aureus* but the DR results showed higher AC_{50} values than for *E. coli* model membranes. Thus the activity against model membranes appears to be opposite to the cell assays. Interestingly, Sánchez-Váquez et al. [26] used POPC/POPG (1:3) as a bacterial membrane model and found that the AMP released more calcein than from POPC/Chol (7:3), suggesting that POPC enhances peptide insertion relative to POPE.

A comparison of the HC_{50} and MIC results against the DR assay suggests that the model membrane mimics used herein are not analogous to RBC, Gram-negative and Gram-positive bacteria (note, however, that the RBC concentration is over 100 times that of the bacterial cells used in the standard assays). The DR results indicate that eukaryotic cell membranes would be more susceptible to the AMP reported herein. The RBC-mimics are neutral or zwitterionic whereas the *E. coli* and *S. aureus* model membranes are negatively charged or anionic (30% and 100%, respectively), possibly causing the positively charged UyCT peptides (net charge +2) to stay on the bilayer surface. In the case of the RBC-mimics, the peptides do not have this attraction to the surface and, therefore, penetrate the membrane bilayer causing dye release. The molecular mechanism responsible for releasing the fluorophore could be pore formation (*e.g.* barrel-stave, carpet-like, toroidal or wormhole pore formation), although further work is required to determine the means.

3.5. DR with peptide combinations

As for single peptides, the amount of leakage for combination of peptides was determined (Fig. 5 and Table 8). In RBC-like membranes, combinations UyCT5 + UyCT1 and UyCT2 + UyCT5 had similar behavior with 100% release at low concentrations. Then UyCT3 + UyCT5 reached 100% release but at higher concentration. UyCT1 + UyCT3 was the least active combination against RBC-mimics reaching only 90% release at higher concentrations than used for the other combinations. This result supports the HC_{50} results determined for peptide combinations (Table 5) where the hemolytic activity for the peptide combination was less than for single peptides (Table 2). Also, the DR results for single peptides showed that all reached 100% release at lower concentrations than for peptide combinations.

For *E. coli*-like membrane, combinations of peptide did not reach 100% release. The most active was UyCT2 + UyCT5 reaching 80%, followed by UyCT1 + UyCT5 with 60% release. UyCT3 + UYCT5 and UyCT1 + UyCT3 were similar, reaching only 30% release. These findings

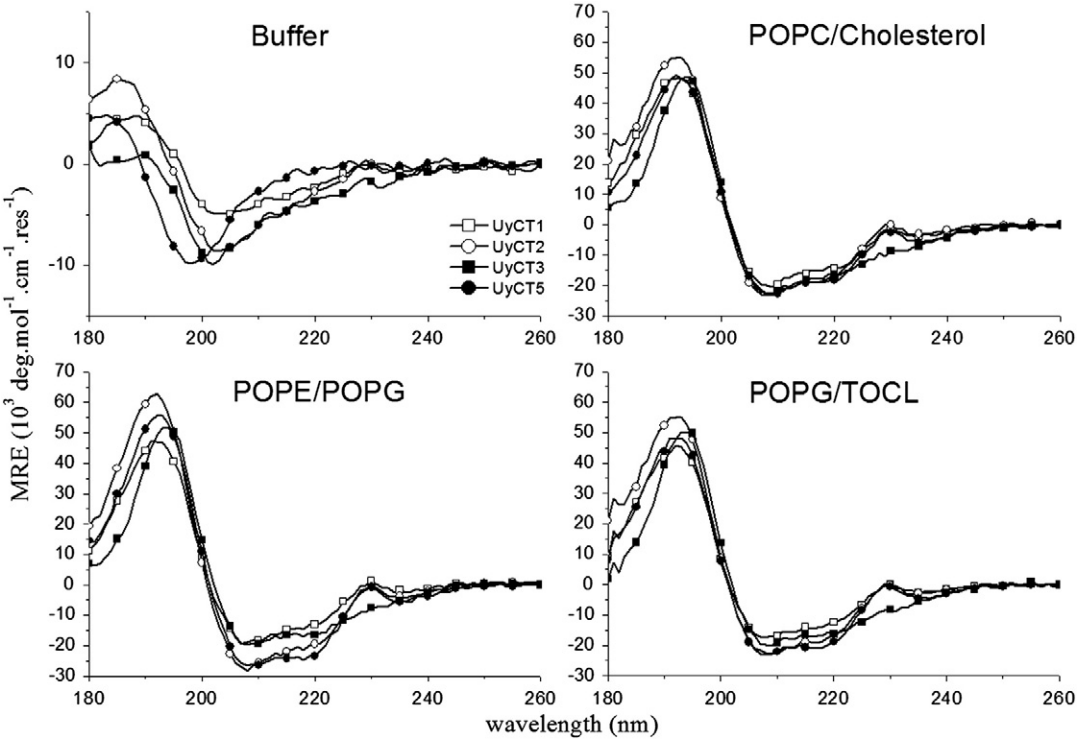

Fig. 2. CD spectra of UyCT peptides in large unilamellar vesicles (LUV). The mean-residue ellipticity (MRE) of 100 nm LUV was obtained using the DICHROWEB website with the ContinLL algorithm and the SMP56 basis-set.

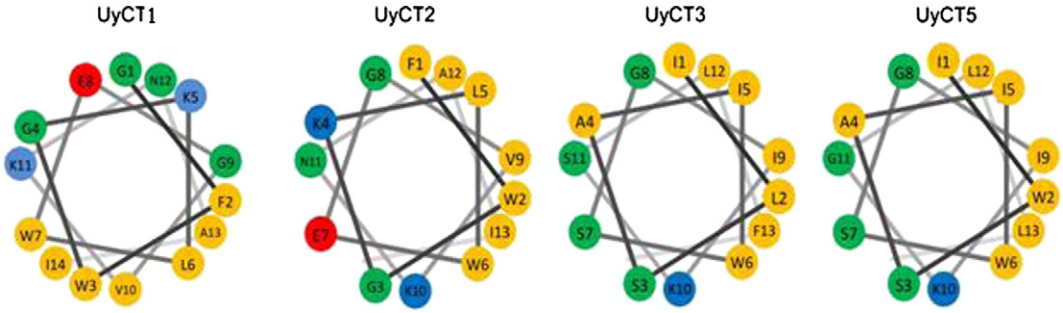

Fig. 3. Helical wheel projection of UyCT peptides: hydrophobic amino acids (yellow) concentrated on one side of the helix and, on the other side, polar (green residues) or hydrophilic/charged amino acids (blue and with acidic residues in red) showing the amphipathic character.

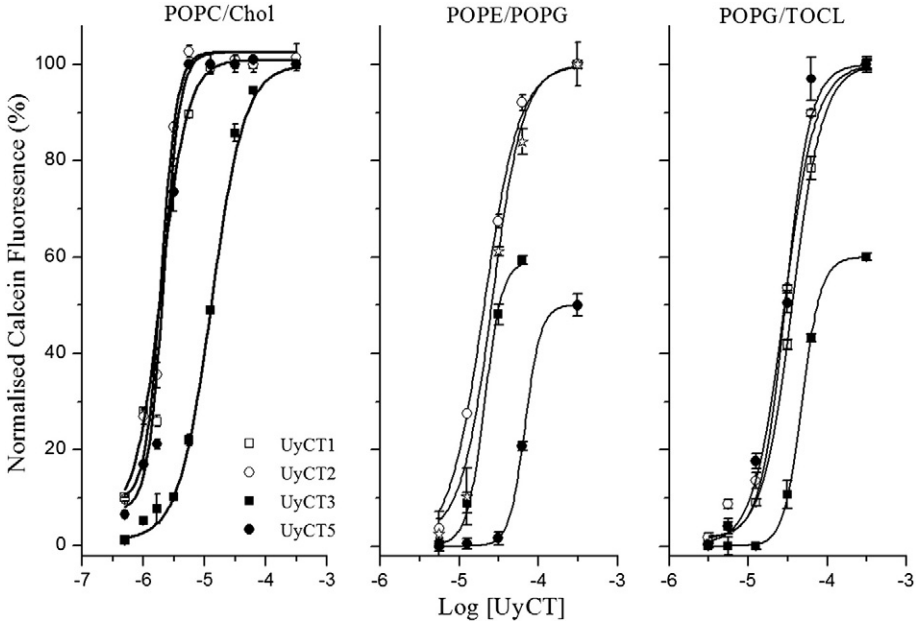

Fig. 4. Dye leakage assay for UyCT peptides fitted with concentration–response equation. Left panel shows RBC-like (POPC/Chol), middle corresponds to *E. coli*-like and right panel to *S. aureus*-like membrane.

do not correlate well with the susceptibility tests where the least active combination was UyCT2 + UyCT5, the one with the highest release in this case. Also, according to MIC values the most active combination for *E. coli* was UyCT3 + UyCT5 which here was the least active combination for dye release. This could be due to the inadequate membrane model (as discussed in the above section, *i.e.*, surface *vs.* insertion) or competition assays with RBC-like and *E. coli*-like membranes should be used to determine peptide preference.

For *S. aureus*-like membranes, combination of peptides reached at the most 70% or 50% dye release. UyCT2 + UyCT5 and UyCT5 + UyCT1 were the more active combinations, while UyCT3 + UyCT5 and UyCT1 + UyCT3 were the least.

Table 7
Parameters obtained from dye release from LUV by UyCT peptides.

Peptide	POPC/Chol 20%[a]		POPE/POPG 7:3[a]		POPG/TOCL 3:2[a]	
	AC_{50} (μM)	n	AC_{50} (μM)	n	AC_{50} (μM)	n
UyCT1	2.1 ± 0.2	2.3 ± 0.4	20.9 ± 5.2	3.9 ± 0.4	36.3 ± 1.0	2.3 ± 0.1
UyCT2	1.9 ± 0.1	3.3 ± 0.4	20.4 ± 0.9	1.9 ± 0.1	29.5 ± 2.0	2.8 ± 0.3
UyCT3	12.9 ± 0.7	1.6 ± 0.1	67.6 ± 0.5	4.4 ± 0.4	47.9 ± 0.3	3.7 ± 0.1
UyCT5	2.1 ± 0.1	3.2 ± 0.3	26.3 ± 1.5	2.2 ± 0.3	28.8 ± 2.2	2.2 ± 0.2

AC_{50} = concentration necessary to produce half of the maximum fluorescence.
n = cooperativity between the peptides to produce the activity.
[a] LUV (100 nm) concentration was fixed at 250 μM with 50% of dye-free LUV.

3.6. Test of D-peptide activity

To confirm membrane targeting by these peptides, D-isomers of UyCT peptides were synthesized and assayed against *Enterococcus faecalis* and *E. coli* control strain, Gram-positive and Gram-negative bacteria, respectively (Table 9). The MIC determined for natural (L-peptides) and D-peptides supports that the mode of action of these peptides is targeting bacterial membranes because the MIC was in the same range of concentrations, in fact, slightly lower for D-peptides, confirming membranes as the target instead of protein receptors or enzymes in the bacteria [36].

4. Conclusion

Gram-negative bacteria, due to their LPS outer membrane, are a challenge for antibiotics but UyCT peptides are active against several strains. In particular, UyCT antimicrobial peptides show potential as new antimicrobials to target infections caused by *A. baumanni* due to the low MIC exhibited towards this strain. Combining peptides enhanced their activity with some synergistic effects without increasing their

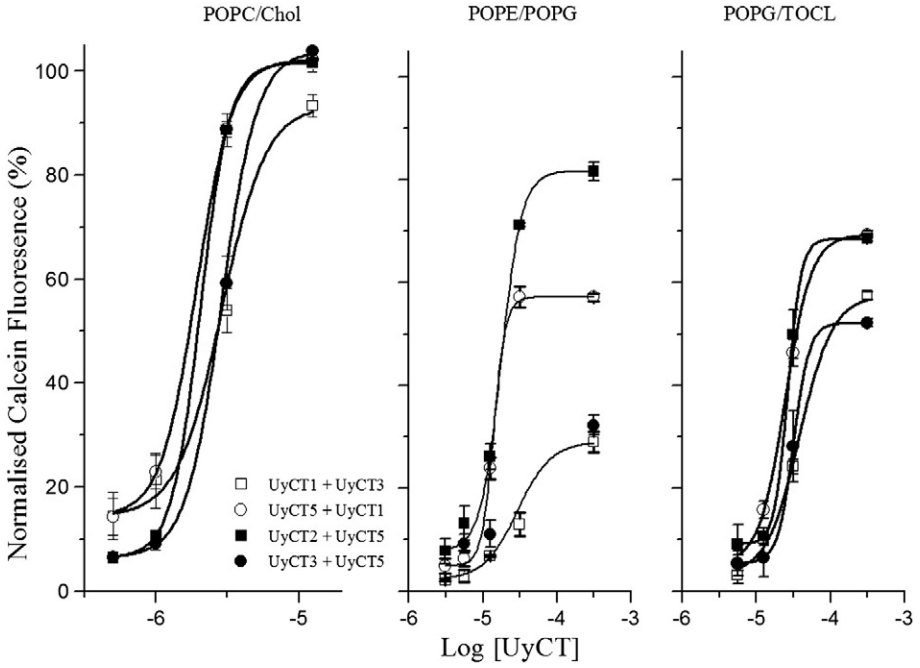

Fig. 5. Dye leakage assays for combination of UyCT peptides fitted with a concentration–response equation. Left panel shows RBC-like membrane (POPC/Chol), middle panel corresponds to *E. coli*-like membranes and right panel to *S. aureus*-like membrane.

Table 8
Parameters obtained from dye release from LUV by peptide combinations.

Peptides	POPC/Chol 20%[a]		POPE/POPG 7:3[a]		POPG/TOCL 3:2[a]	
	AC_{50} (μM)	n	AC_{50} (μM)	n	AC_{50} (μM)	n
UyCT1 + UyCT3	4.1 ± 0.2	1.0 ± 0.1	44.6 ± 7.7	1.1 ± 0.1	42.5 ± 1.9	1.4 ± 0.1
UyCT5 + UyCT1	1.5 ± 0.1	2.5 ± 0.3	13.7 ± 1.4	2.9 ± 0.8	22.4 ± 0.7	2.0 ± 0.1
UyCT2 + UyCT5	1.8 ± 0.2	3.4 ± 0.5	15.9 ± 2.3	2.1 ± 0.5	21.9 ± 3.1	2.6 ± 0.7
UyCT3 + UyCT5	2.9 ± 0.2	2.1 ± 0.3	–	–	29.8 ± 3.8	1.9 ± 0.4

AC_{50} = concentration necessary to produce half of the maximum fluorescence.
n = cooperativity between the peptides to produce the activity.
[a] LUV (100 nm) concentration was fixed at 250 μM with 50% dye-free LUV.

hemolytic effect, which enhances the therapeutic index. The HC_{50} results indicate the need to modify their sequence/structure to improve their therapeutic index (lower their toxicity and improve their potency) through competitive assays by increasing their affinity for model bacterial membranes and decreasing that for eukaryotic membranes.

Acknowledgements

This work was supported by grants from the Dirección General de Asuntos del Personal Academico, UNAM (IN200113), awarded to LDP; the Struan Sutherland Fund to AVRU, The University of Melbourne; and the Australian Research Council to FS. KLR gratefully acknowledges PhD scholarship from CONACyT and The Hugh Williamson Foundation, Museum Victoria.

Table 9
Minimal inhibitory concentration (MIC) for L- and D-peptides.

Microorganism	MIC (μM)							
	L-peptides				D-peptides			
	UyCT1	UyCT2	UyCT3	UyCT5	UyCT1	UyCT2	UyCT3	UyCT5
E. faecalis ATCC 29212	31.25	125	15.6	7.8	15.6	125	31.25	7.8
E. coli ATCC 25922	14	32	25	25	8	14	16	16

The authors acknowledge Dr Veronica Quintero-Hernández for support during structural determination of the peptides used here.

Appendix A. Supplementary data

Supplementary data to this article can be found online at http://dx.doi.org/10.1016/j.bbamem.2013.10.022.

References

[1] K. Lewis, Platforms for antibiotic discovery, Nat. Rev. Drug Discov. 12 (2013) 371–387.
[2] Y. Li, Q. Xiang, Q. Zhang, Y. Huang, Z. Su, Overview on the recent study of antimicrobial peptides: origins, functions, relative mechanisms and application, Peptides 37 (2012) 207–215.
[3] G. Wang, X. Li, Z. Wang, APD2: the updated antimicrobial peptide database and its application in peptide design, Nucleic Acids Res. 37 (2009) D933–D937.
[4] J.H. Bowie, F. Separovic, M.J. Tyler, Host-defense peptides of Australian anurans. Part 2. Structure, activity, mechanism of action, and evolutionary significance, Peptides 37 (2012) 174–188.
[5] P. Bulet, R. Stöcklin, L. Menin, Anti-microbial peptides: from invertebrates to vertebrates, Immunol. Rev. 198 (2004) 169–184.
[6] G. Corzo, P. Escoubas, E. Villegas, K.J. Barnham, W. He, R.S. Norton, T. Nakajima, Characterization of unique amphipathic antimicrobial peptides from venom of the scorpion *Pandinus imperator*, Biochem. J. 359 (2001) 35–45.
[7] H. Steiner, D. Hultmark, A. Engstrom, H. Bennich, H.G. Boman, Sequence and specificity of two antibacterial proteins involved in insect immunity, Nature 292 (1981) 246–248.
[8] J.M.A. Cerón, J. Contreras-Moreno, E. Puertollano, G.A. De Cienfuegos, M.A. Puertollano, M.A. De Pablo, The antimicrobial peptide cecropin A induces

caspase-independent cell death in human promyelocytic leukemia cells, Peptides 31 (2010) 1494–1503.
[9] R. Smith, F. Separovic, T.J. Milne, A. Whittaker, F.M. Bennett, B.A. Cornell, A. Makriyannis, Structure and orientation of the pore-forming peptide, melittin, in lipid bilayers, J. Mol. Biol. 241 (1994) 456–466.
[10] J. Orivel, V. Redeker, J.P. Le Caer, F. Krier, A.M. Revol-Junelles, A. Longeon, A. Chaffotte, A. Dejean, J. Rossier, Ponericins, new antibacterial and insecticidal peptides from the venom of the ant Pachycondyla goeldii, J. Biol. Chem. 276 (2001) 17823–17829.
[11] G. Corzo, E. Villegas, F. Gómez-Lagunas, L.D. Possani, O.S. Belokoneva, T. Nakajima, Oxyopinins, large amphipathic peptides isolated from the venom of the wolf spider Oxyopes kitabensis with cytolytic properties and positive insecticidal cooperativity with spider neurotoxins, J. Biol. Chem. 277 (2002) 23627–23637.
[12] L. Kuhn-Nentwig, J. Müller, J. Schaller, A. Walz, M. Dathe, W. Nentwig, Cupiennin 1, a new family of highly basic antimicrobial peptides in the venom of the spider Cupiennius salei (Ctenidae), J. Biol. Chem. 277 (2002) 11208–11216.
[13] A. Mor, Isolation, amino acid sequence, and synthesis of dermaseptin, a novel antimicrobial peptide of amphibian skin, Biochemistry 30 (1991) 8824–8830.
[14] T.L. Pukala, M.P. Boland, J.D. Gehman, L. Kuhn-Nentwig, F. Separovic, J.H. Bowie, Solution structure and interaction of cupiennin 1a, a spider venom peptide, with phospholipid bilayers, Biochemistry 46 (2007) 3576–3585.
[15] A. Torres-Larios, G.B. Gurrola, F.Z. Zamudio, L.D. Possani, Hadrurin, a new antimicrobial peptide from the venom of the scorpion Hadrurus aztecus, Eur. J. Biochem. 267 (2000) 5023–5031.
[16] L. Dai, A. Yasuda, H. Naoki, G. Corzo, M. Andriantsiferana, T. Nakajima, IsCT, a novel cytotoxic linear peptide from scorpion Opisthacanthus madagascariensis, Biochem. Biophys. Res. Commun. 286 (2001) 820–825.
[17] E.C.N. Silva, T.S. Camargos, A.Q. Maranhão, I. Silva-Pereira, L.P. Silva, L.D. Possani, E.F. Schwartz, Cloning and characterization of cDNA sequences encoding for new venom peptides of the Brazilian scorpion *Opisthacanthus cayaporum*, Toxicon 54 (2009) 252–261.
[18] X.C. Zeng, G. Corzo, R. Hahin, Scorpion venom peptides without disulfide bridges, IUBMB Life 57 (2005) 13–21.
[19] X.-C. Zeng, L. Zhou, W. Shi, X. Luo, L. Zhang, Y. Nie, J. Wang, S. Wu, B. Cao, H. Cao, Three new antimicrobial peptides from the scorpion Pandinus imperator, Peptides 45 (2013) 28–34.
[20] R.E. Hancock, H.G. Sahl, Antimicrobial and host-defense peptides as new antiinfective therapeutic strategies, Nat. Biotechnol. 24 (2006) 1551–1557.
[21] K. Luna-Ramírez, V. Quintero-Hernández, L. Vargas-Jaimes, C.V.F. Batista, K.D. Winkel, L.D. Possani, Characterization of the venom from the Australian scorpion Urodacus yaschenkoi: molecular mass analysis of components, cDNA sequences and peptides with antimicrobial activity, Toxicon 63 (2013) 44–54.
[22] J. Silva, C. Aguilar, G. Ayala, M.A. Estrada, U. Garza-Ramos, R. Lara-Lemus, L. Ledezma, TLA-1: a new plasmid-mediated extended-spectrum β-lactamase from *Escherichia coli*, Antimicrob. Agents Chemother. 44 (2000) 997–1003.
[23] J. Silva-Sanchez, F. Reyna-Flores, M.E. Velázquez-Meza, T. Rojas-Moreno, A. Benitez-Diaz, A. Sanchez-Perez, *In vitro* activity of tigecycline against ESBL-producing Enterobacteriaceae and MRSA clinical isolates from Mexico: multicenter study, Diagn. Microbiol. Infect. Dis. 70 (2011) 270–273.
[24] J. Silva, R. Gatica, C. Aguilar, Z. Becerra, U. Garza-Ramos, M. Velázquez, G. Miranda, B. Leaños, F. Solórzano, G. Echániz, Outbreak of infection with extended-spectrum beta-lactamase-producing *Klebsiella pneumoniae* in a Mexican hospital, J. Clin. Microbiol. 39 (2001) 3193–3196.
[25] U. Garza-Ramos, R. Morfin-Otero, H.S. Sader, R.N. Jones, E. Hernández, E. Rodriguez-Noriega, A. Sanchez, B. Carrillo, S. Esparza-Ahumada, J. Silva-Sanchez, Metallo-beta-lactamase gene bla(IMP-15) in a class 1 integron, In95, from *Pseudomonas aeruginosa* clinical isolates from a hospital in Mexico, Antimicrob. Agents Chemother. 52 (2008) 2943–2946.
[26] L. Sánchez-Vásquez, J. Silva-Sanchez, J.M. Jiménez-Vargas, A. Rodríguez-Romero, C. Muñoz-Garay, M.C. Rodríguez, G.B. Gurrola, L.D. Possani, Enhanced antimicrobial activity of novel synthetic peptides derived from vejovine and hadrurin, Biochim. Biophys. Acta, Gen. Subj. 1830 (2013) 3427–3436.
[27] A. Lobley, L. Whitmore, B.A. Wallace, DICHROWEB: an interactive website for the analysis of protein secondary structure from circular dichroism spectra, Bioinformatics 18 (2002) 211–212.
[28] S.W. Provencher, J. Glockner, Estimation of globular protein secondary structure from circular dichroism, Biochemistry 20 (1981) 33–37.
[29] R.L. Anderson, S. Davis, An organic phosphorus assay which avoids the use of hazardous perchloric acid, Clin. Chim. Acta 121 (1982) 111–116.
[30] R.J. Tallarida, Drug synergism: its detection and applications, J. Pharmacol. Exp. Ther. 298 (2001) 865–872.
[31] R.J. Tallarida, Revisiting the isobole and related quantitative methods for assessing drug synergism, J. Pharmacol. Exp. Ther. 342 (2012) 2–8.
[32] S.M. Tham, J.A. Angus, E.M. Tudor, C.E. Wright, Synergistic and additive interactions of the cannabinoid agonist CP55,940 with μ opioid receptor and α 2-adrenoceptor agonists in acute pain models in mice, Br. J. Pharmacol. 144 (2005) 875–884.
[33] M.-A. Sani, T.C. Whitwell, F. Separovic, Lipid composition regulates the conformation and insertion of the antimicrobial peptide maculatin 1.1, Biochim. Biophys. Acta 1818 (2012) 205–211.
[34] T.C.B. Vogt, B. Bechinger, The interactions of histidine-containing amphipathic helical peptide antibiotics with lipid bilayers. the effects of charges and pH, J. Biol. Chem. 274 (1999) 29115–29121.
[35] James Darnell, Harvey Lodish, D. Baltimore, Molecular Cell Biology, second ed. Scientific American Books, New York, USA, 1990.
[36] D. Wade, A. Boman, B. Wahlin, C.M. Drain, D. Andreu, H.G. Boman, R.B. Merrifield, All-D amino acid-containing channel-forming antibiotic peptides, Proc. Natl. Acad. Sci. U. S. A. 87 (1990) 4761–4765.
[37] J. Seelig, Titration calorimetry of lipid–peptide interactions, Biochim. Biophys. Acta, Rev. Biomembr. 1331 (1997) 103–116.
[38] J. Tellinghuisen, Statistical Error in Isothermal Titration Calorimetry, vol. 383, 2004, pp. 245–282.